

Experimental study on precast beam-column connections with continuity reinforcement for negative bending moments

Análise experimental de ligações viga-pilar pré-moldadas com armadura de continuidade para momentos fletores negativos



G. M. S. ALVA^a
alva_gerson@yahoo.com.br
<https://orcid.org/0000-0002-2528-5757>

M. M. S. LACERDA^a
maiza_mz@hotmail.com
<https://orcid.org/0000-0001-5693-971X>

T. J. SILVA^a
tjsilva@gmail.com
<https://orcid.org/0000-0002-2862-0645>

Abstract

In this paper, an experimental investigation is presented on semi-rigid interior beam-to-column connections constituted by precast concrete beams supported on precast concrete column corbels and bending continuity reinforcement bars for bending negative moments. The main purpose of this paper was to analyze the influence of vertical interface grout filling between the corbel and the beam and the position of the bending continuity reinforcement bars (crossing only the column or crossing only the slab) on the behavior of this type of connection. Tests on eight specimens were performed. It was noticed that the vertical interface grout filling contributed to increase both rotational flexural stiffness and flexural strength capacity of the connections when compared to the connections without grout filling. It was also noticed that in the specimens in which the continuity bars crossed only the column, the rotational flexural stiffness was higher. For these last ones, coefficients k and β for predicting the secant stiffness by simplified expression present in Brazilian Code NBR 9062 were evaluate from experimental results. These evaluated coefficients may be regarded as indicative values for structural designers and helpful for future researches.

Keywords: precast concrete structures, precast beam-column connections, semirigid connections, structural analysis.

Resumo

Neste trabalho apresenta-se um estudo experimental de ligação viga-pilar semirrígida de pilar intermediário constituída de vigas de concreto pré-moldadas apoiadas em consolos de concreto pré-moldado, com presença de armaduras de continuidade resistentes ao momento fletor negativo. O presente trabalho teve como objetivo principal verificar a influência do preenchimento de graute na interface vertical entre o consolo e a viga e a posição da armadura de continuidade (passante somente no pilar e passante somente nas lajes). Foram ensaiados no total oito protótipos. Verificou-se que o preenchimento de graute na interface vertical consolo-viga contribuiu para aumentar tanto a rigidez e quanto a resistência da ligação à flexão quando à comparada a ligação sem o preenchimento desse graute. Verificou-se também que nos protótipos em que as armaduras de continuidade passaram somente no pilar a rigidez à flexão da ligação foi maior. Para estas tipologias de ligação, foram obtidos, a partir dos resultados experimentais, os coeficientes k e β presentes na expressão simplificada da NBR 9062 para o cálculo da rigidez secante. Os valores calculados para esses coeficientes podem servir de valores indicativos e orientativos para projetistas estruturais e para futuras pesquisas.

Palavras-chave: estruturas de concreto pré-moldado, ligações viga-pilar pré-moldadas, ligações semirrígidas, análise estrutural.

^a Universidade Federal de Uberlândia, Faculdade de Engenharia Civil, Uberlândia, MG, Brasil.

1. Introduction

The study of the connections between precast concrete structural members is of great importance for the development and execution of design, since the performance of the precast concrete structural system is directly related to the performance of their connections, affecting both the local behavior of the adjacent members and the global behavior of the structure.

In framed structural systems with precast members, the beam-column connections subjected to bending moments are classified as rigid, semi-rigid or pinned connections, depending on the bending moment mobilized and transferred among its members. The classification and quantification of the flexural stiffness in beam-column connections are important for structural analysis and design of the structure.

In codes overall, the classification of connections depends on the knowledge of rotational stiffness, which depends on the characteristics of the typology of the connection. In general, rotational stiffness should be obtained based on experimental results or through analytical models, which need to be calibrated or validated experimentally. In the last three decades, there have been international experimental studies on different types of beam-column connections [1-14], whose typologies analyzed were chosen mainly due to their concern with behavior under seismic loads.

In Brazil, research involving semi-rigid connections began just over two decades ago [15-25]. In Miotto [17], Souza [18], Baldissera [19], Kataoka [20] and Hadade [25], experimental results of beam-column connections with continuity reinforcement for negative bending moments can be found.

In the context of the present paper, it is appropriate to highlight the tests of Miotto's connections [17], in which the precast beams (dapped-end beams) were supported by concrete corbel and fixed by steel dowels on it. In these connections there was no grout filling between the corbel interface and the lower vertical face of the beam. Half of the continuity reinforcement crossed the column and the other half was placed in the slab. On the other hand, Kataoka [20] also presents two types of beam-column connections with precast beams supported by concrete corbels. In one connection, the continuity reinforcement was fully placed crossing the column; at the other connection, half of the continuity reinforcement crossed the column and the remaining half was distributed in the slab.

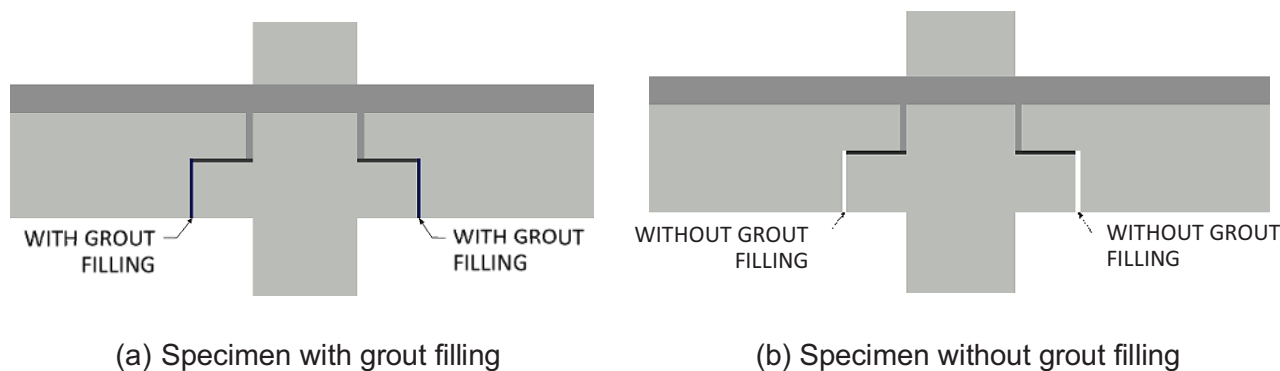


Figure 2

Grouting filling in the vertical interface between corbel and beam

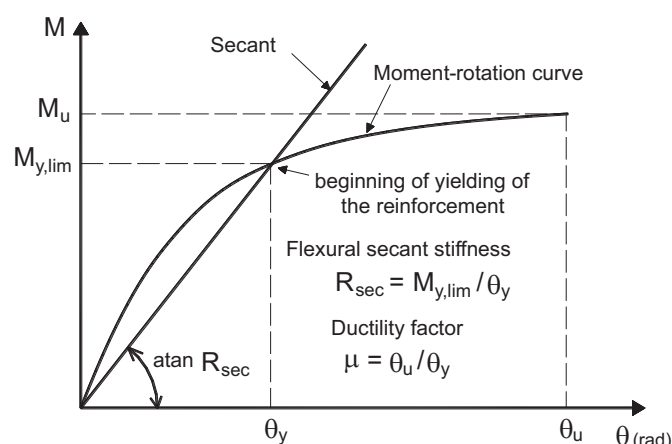


Figure 1

Moment-rotation curve of a beam-column connection: NBR 9062 [27]

This paper presents results of experimental studies conducted by Lacerda [26] about the behavior of four types of precast beam-column connections that can be used in the construction of structures with more than one story, such as factory constructions, industries, and residential buildings. The types of investigated beam-column connections are designed for negative bending moments and are composed of continuity reinforcement, precast beam supported by precast column corbel and fixed by steel dowels and grout filling at the beam and column interface.

The main goal of Lacerda [26] was to evaluate the behavior of the connections under the influence of the filling the lower interface between the beam and the corbel (with or without grout) and the influence of the position of the continuity reinforcement (crossing only the column or only the slab). In order to evaluate the flexural stiffness for negative moments of the connections, it was necessary to obtain experimentally the moment-rotation curves and the secant stiffness of the studied connections.

ABNT NBR 9062 [27] presents a simplified expression for obtaining the secant stiffness R_{sec} (Figure 1) for six connection typologies. The prediction of the secant stiffness allows the consideration of the

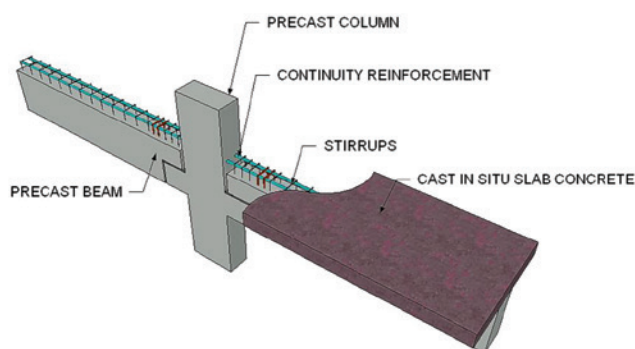


Figure 3
Specimens with continuity reinforcement crossing the column (PC and PS)

deformability (rotational) of the beam-column connections in simplified linear analysis, useful to obtain internal forces and displacements in the structural system. However, it should be noted that the expression indicated in NBR 9062 [27] for obtaining secant stiffness does not include the types of connections investigated in this paper. Thus, as an additional contribution of this paper, it were obtained (for two types of connection) the coefficients k and $e \beta$ present in the simplified expression of NBR 9062 [27] for the prediction of the secant stiffness, from the experimental results obtained by Lacerda [26].

2. Experimental tests

2.1 Characteristics of the beam-column connections specimens

The experimental program was performed by Lacerda [26] and consisted of the investigation of interior precast beam-column connections specimens under negative bending moment. The main goals of the experimental program were to verify the influence of two variables:

- Vertical grout filling at the interface between corbel and beam (Figure 2);
- Position of the continuity reinforcement (crossing only the column or only the slab (Figures 3 and 4).

Four variations of specimens were tested (two for each variation). Thus, eight specimens were tested. Table 1 presents the nomenclature used for the specimens.

Figure 3 shows the connections where continuity reinforcement only pass through the column (PC and PS) and Figure 4, the

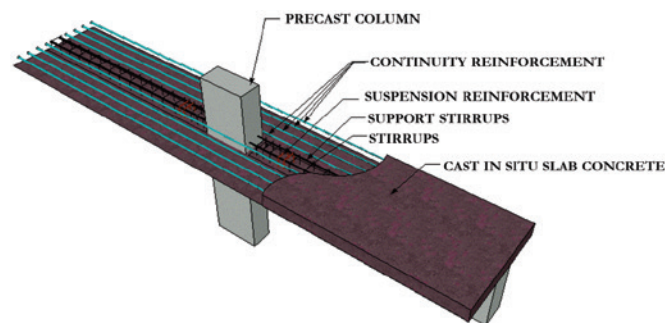


Figure 4
Specimens with continuity reinforcement crossing the slab (LC and LS)

connections where continuity reinforcement only pass through the slab (LC and LS). For all specimens, the total area of continuity reinforcement was the same (4.02 cm^2).

As shown in Figures 3 and 4, each specimen is composed of a precast column, two precast cantilever beams supported by column corbels and seated on cushion of grout and the presence of steel dowel. The specimens also present cast-in-situ concrete slab, grout filling at the interface between the column and beam, continuity reinforcement and whether or not the grout has been fulfilled at the vertical interface between the corbel and the beam. The geometric characteristics of all specimens and the details of the steel dowel positioning are shown, respectively, in Figures 5 and 6.

Details of the reinforcement columns, corbels, beams and slabs are shown in Figures 7 to 11.

2.2 Mechanical properties of the materials

For the construction of the precast beams and columns, a 40 MPa compressive strength for the concrete was specified. For the cast-in-situ concrete slab, a 25 MPa compressive strength was specified. Two CA50 steel bars of 16 mm diameter were used as continuity reinforcement, totaling an area of 4.02 cm^2 in each specimen. This reinforcement was cast in concrete slab, providing the flexural strength capacity for the connection (negative bending moment). The corbels and beams were left with holes for fixing the steel dowels (CA60 steel bars of 9.5 mm diameter). Later these holes were filled with grout. For the filling of grout at the vertical interface (between corbel and beam: PC and LC specimens) a self-compacting shrinkage compensated grout of 40 MPa compressive strength was specified.

Table 1

Nomenclature of the specimens

Specimen	Continuity reinforcement	Variable	
		Filling with grout	
			Quantity
PS	Only crossing the column	Without	2
PC	Only crossing the column	With	2
LS	Only crossing the slab	Without	2
LC	Only crossing the slab	With	2

PS – Specimen without grout filling; PC – Specimen with grout filling; LS – Specimen without grout filling; LC – Specimen with grout filling

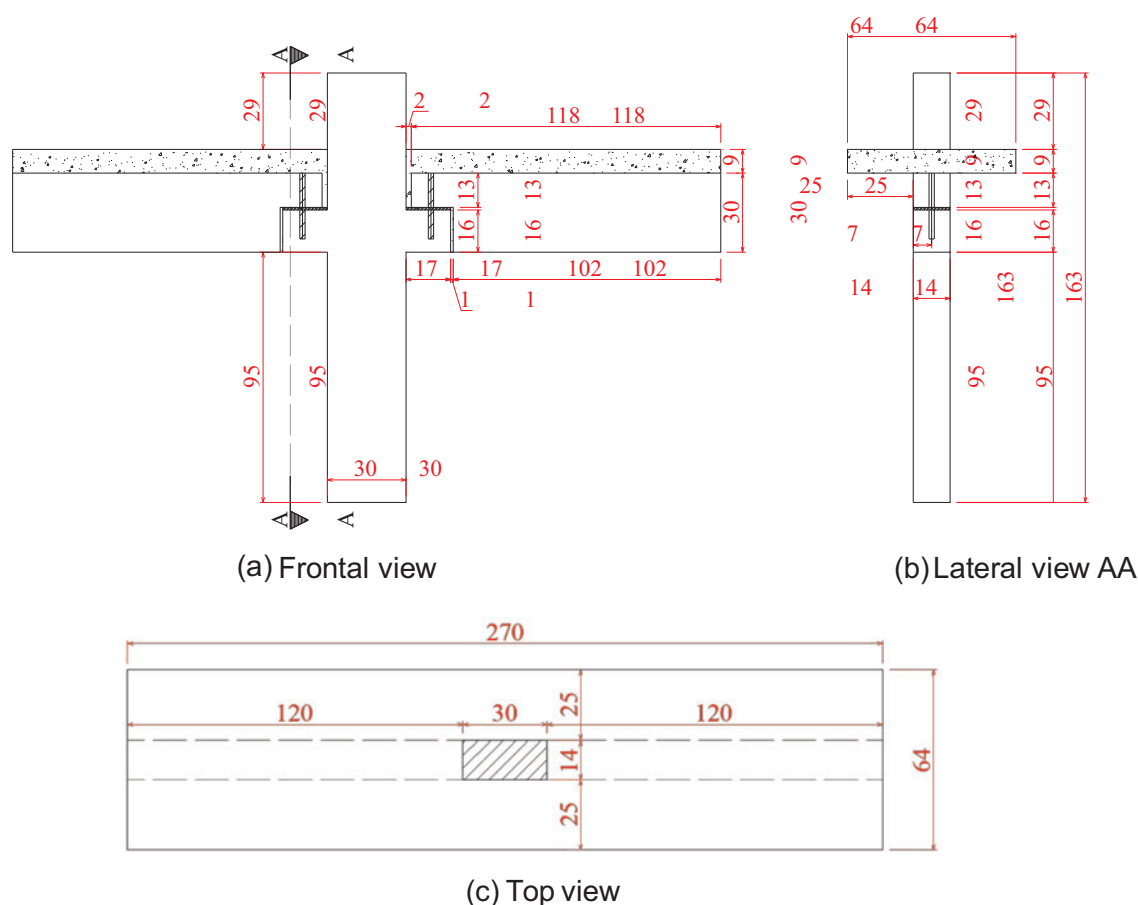


Figure 5
Geometric characteristics of the specimens (dimensions in cm)

Tests on cylinder specimens (100 mm x 200 mm) were performed to control concrete/grout compressive strength, according to the Brazilian standards. Concrete compressive strength was approximately 48 MPa for precast beams and columns and 35 MPa for concrete slabs. Grout compressive strength was 50 MPa. The

yielding and ultimate strength of the continuity reinforcement are approximately 600 MPa and 730 MPa, respectively.

2.3 Construction of the specimens

A steel shoring system was used for positioning and leveling the precast elements and for supporting the slab formwork.

The sequence of steps for the construction of each specimen was:

- 1 – Positioning of the column;
- 2 – Insertion of the steel dowels and filling corbel holes with grout;
- 3 – Setting the cushion of grout on the corbels;
- 4 – Setting the beams on the corbels;
- 5 – Filling vertical space between corbel and beam with grout for specimens PC e LC;
- 6 – Setting up slab formwork;
- 7 – Filling spaces between beam and column with grout;
- 8 – Insertion of the continuity reinforcement bars and slab reinforcement bars;
- 9 – Filling the column holes for the continuity reinforcement with grout;
- 10 – Casting of the concrete slabs.

Figure 12 illustrates the lifting procedure of the columns and beams and how the steel dowels and the cushion of grout of the beams

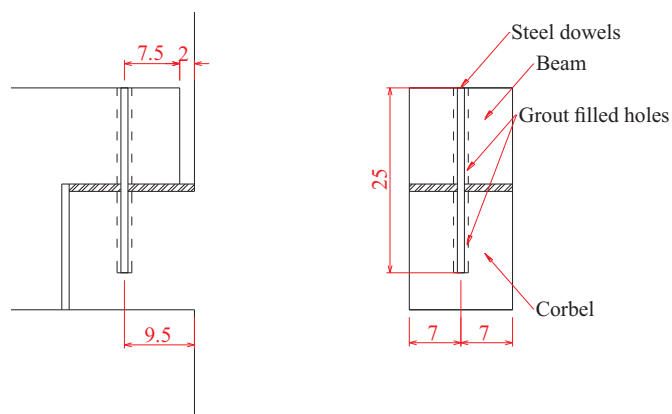


Figure 6
Position of the steel dowels (dimensions in cm)

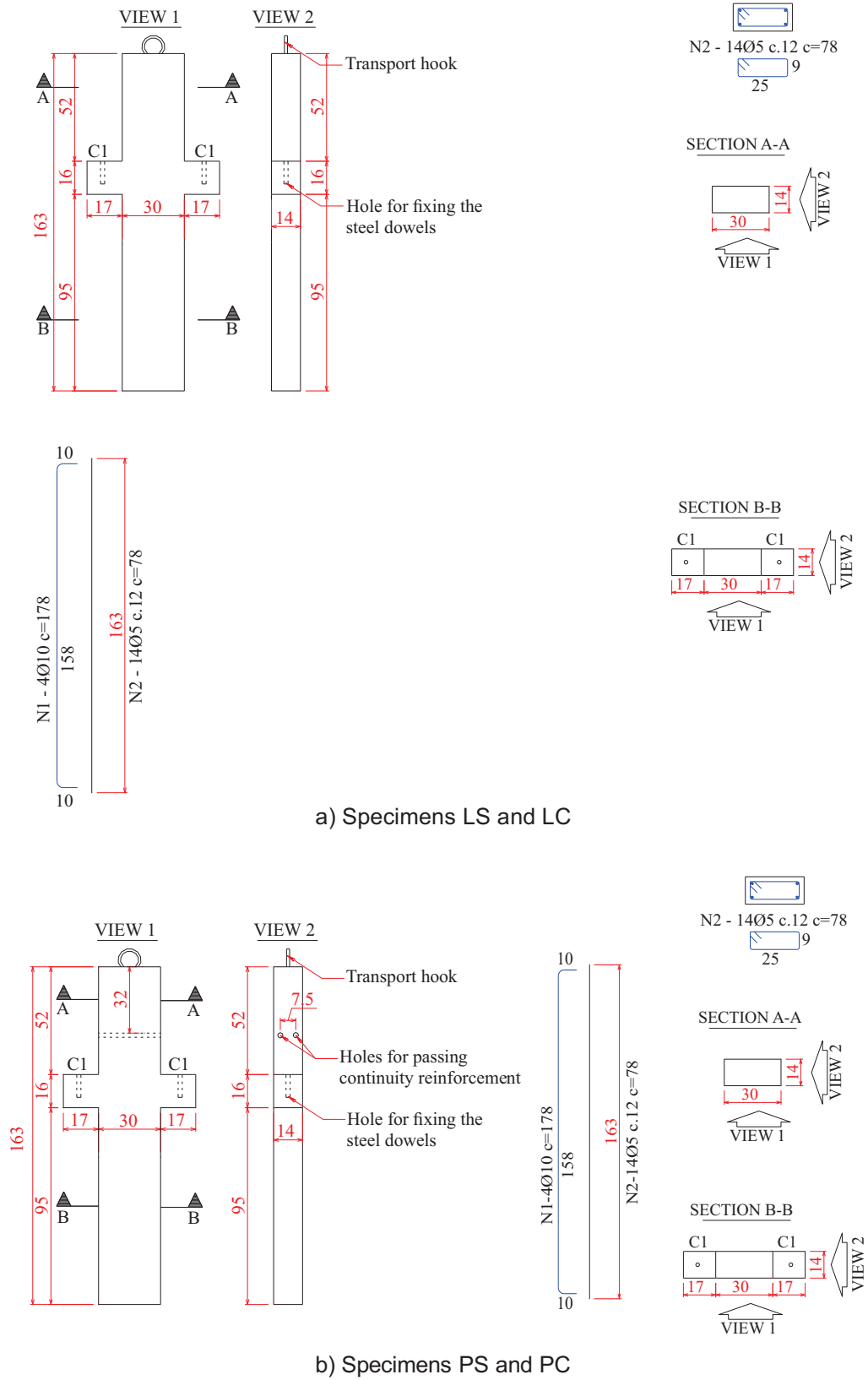


Figure 7
Details of the columns (length dimensions in cm)

installation were performed. Figure 13 illustrates how the beam-to-column union was performed, the vertical grouting of the bottom face of the beam with column corbel (in PC and LC specimens), as well as it illustrates the detail of the continuity reinforcement crossing the column (in PC specimens).

2.4 Test setup and procedures

A hydraulic jacket (actuator with 500 kN load capacity) was used to induce negative bending moments in the specimens. The actuator applied to the base of the column increasing forces (F) upwards (according to Figure 14). Through the reaction structure (Figure 15), forces (F/2) were applied to the ends of each beam. The column was supported on a steel plate above the actuator for distribution of the load over the cross section (column). Guides fixed to the reaction frame were used to provide lateral stability of the specimens during the test. For the linear distribution of the load on the slab ends loading steel bars were centralized over the elastomeric bearings at the points of the reaction forces - 1.07 meters from the column faces. Above each steel bar there were a plate, steel devices (to increase the available distance between the top of the column and reaction structure) and the load cell to capture the reaction force at the ends of the beams. Figure 15 illustrates the test setup for all specimens. Displacement transducers (LVDTs) were used to measure: i) beam deflections at point of load; ii) to determine relative rotation between beam and column (both sides of the column); iii) to monitor the connection zone. Figure 16 indicates the position of the displacement transducers in the specimens. Figure 17 gives a general view of the equipment used in the tests.

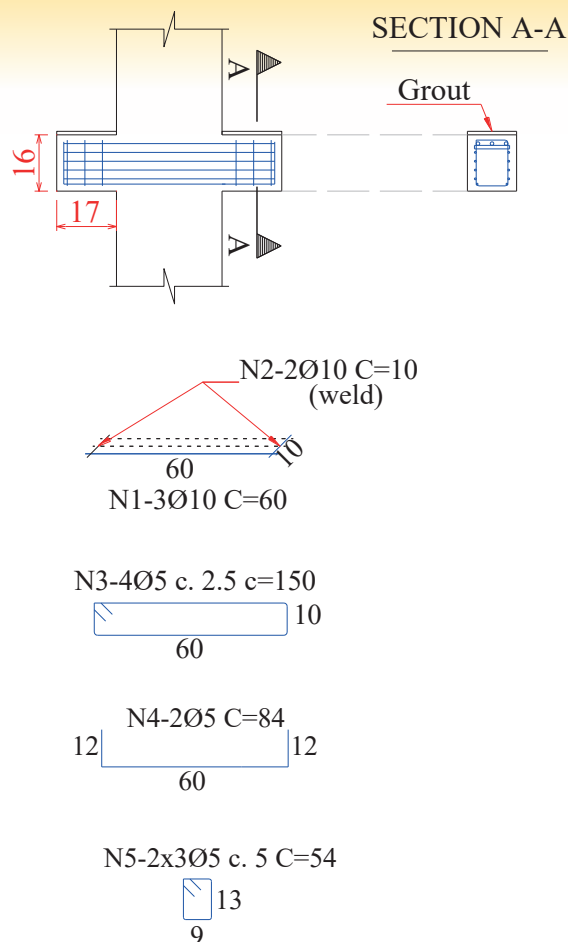


Figure 8
Details of the corbels for all specimens (length dimensions in cm)

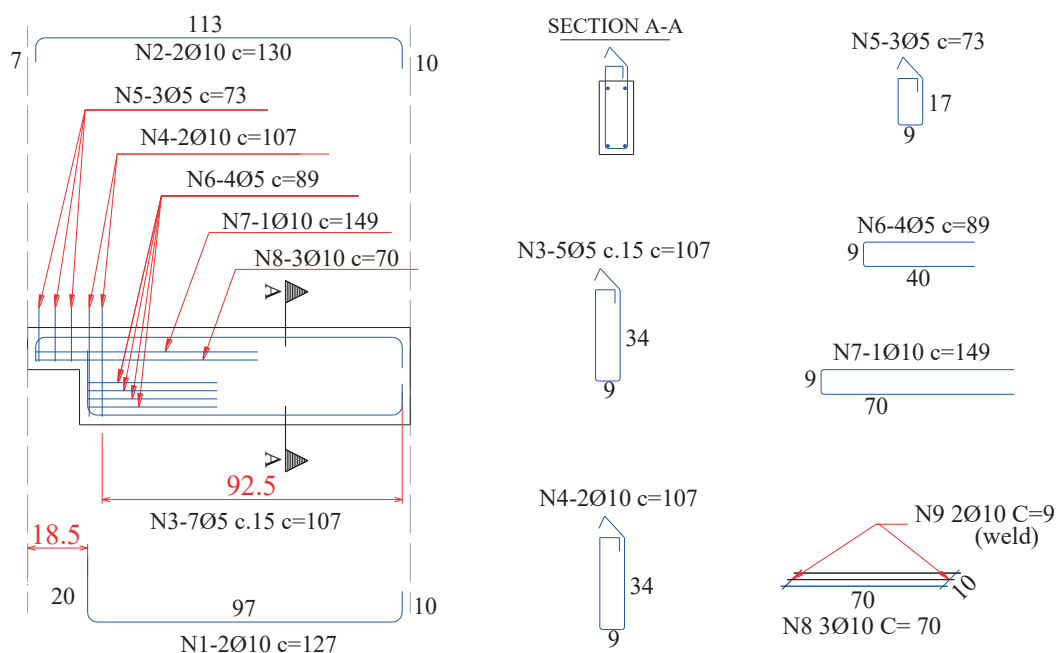


Figure 9
Details of the beams for all specimens (length dimensions in cm)

3. Experimental results analysis

3.1 Cracking

The cracking was concentrated on the cast-in-situ slabs for all speci-

mens. Figures 18 and 19 show the cracking pattern in the slabs of the tested connections. It can be noticed that the distribution of these cracks is approximately symmetrical and parallel to the smallest column face. For all specimens, cracks appeared on the column slab interfaces mainly toward the least direction of the column. In specimens with crossing slab continuity reinforcement (LC and

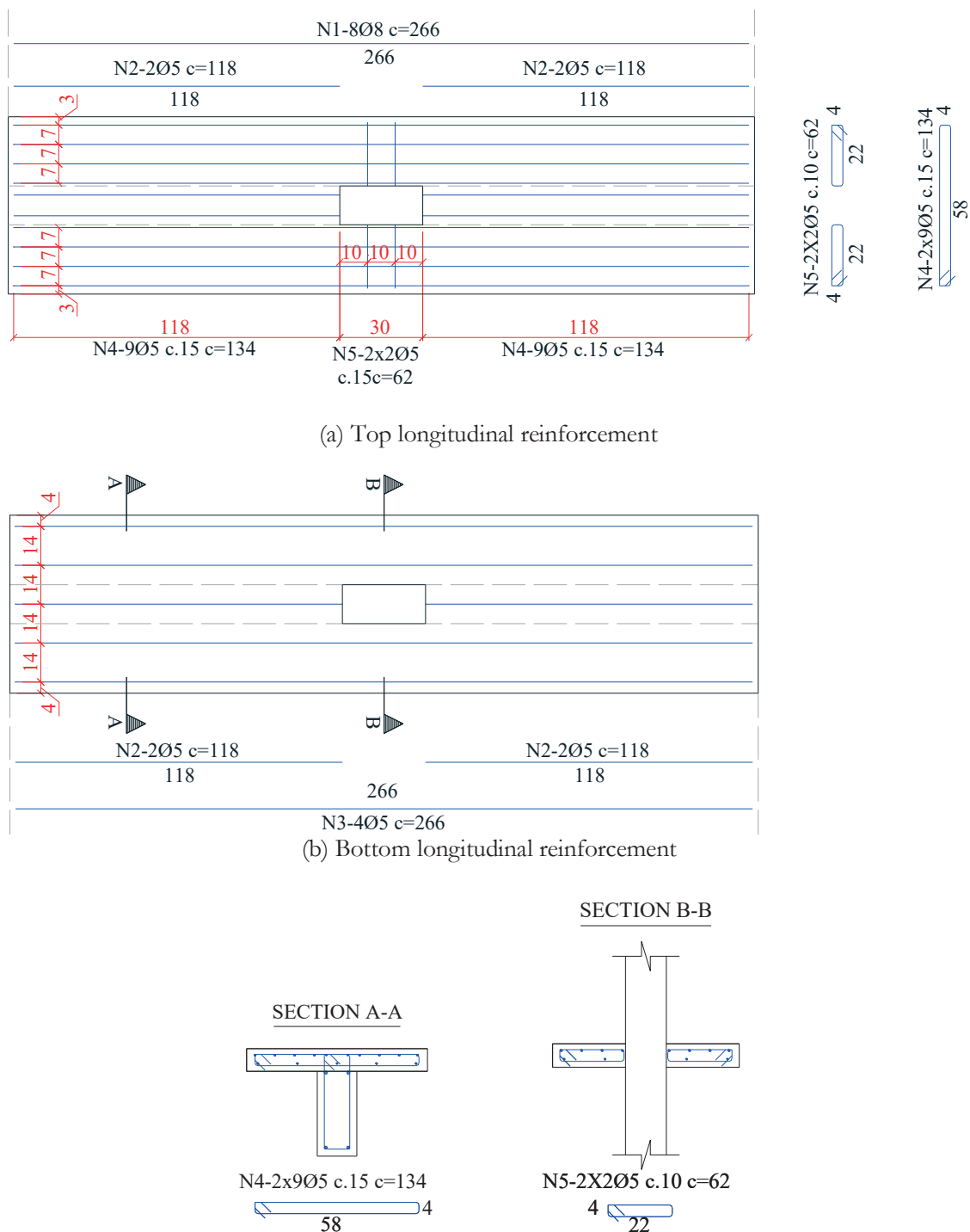
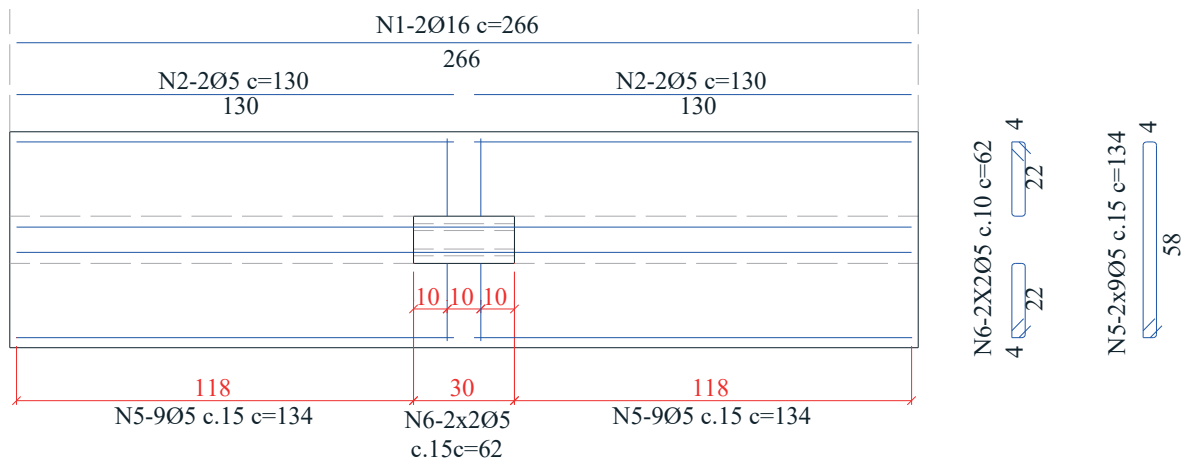
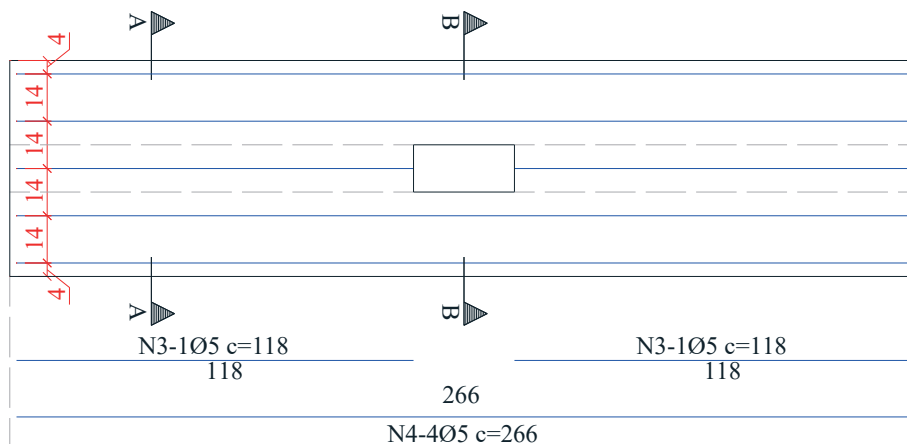


Figure 10
Details of the slabs: specimens LC and LS (length dimensions in cm)



(a) Top longitudinal reinforcement



(b) Bottom longitudinal reinforcement

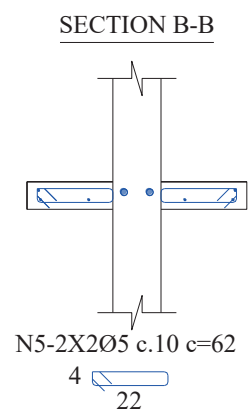
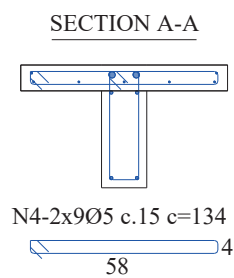


Figure 11
Details of the slabs: specimens PC and PS (length dimensions in cm)



Figure 12
Lifting of the precast elements, steel dowel and cushion of grout of the beams



Figure 13
Setting beams on corbels, vertical grouting (PC and LC) and continuity reinforcement crossing the column (PC)

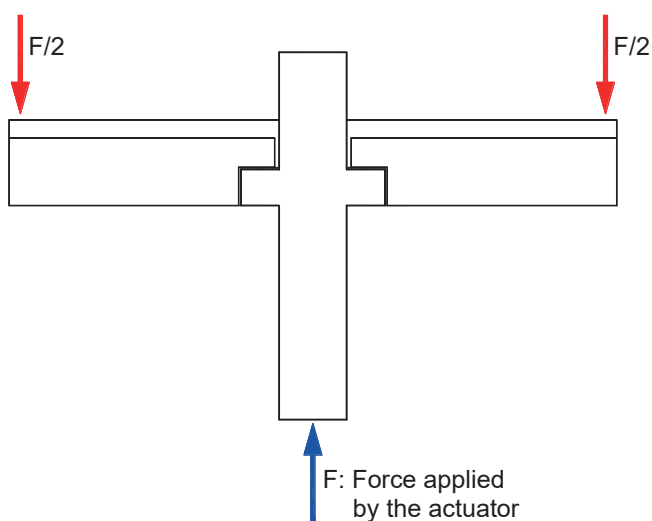


Figure 14
Loading applied to the specimens

LS), it was observed that there was a greater crack distribution (lower cracking spacing) during loading in relation to specimens with crossing column reinforcement (PC and PS), as shown in Figures 18 and 19. This fact is related to the different diameters of the continuity reinforcement bars used in the specimens, since the diameter of a steel bar in tension influences the spacing between flexural cracks.

3.2 Flexural strength

Table 2 shows the maximum values of the applied loads to the beam ends ($F/2$) by the reaction structure. From these forces and knowing that the distance between the point of application of the loads and the face of the column is 1.07 m, the ultimate moment (flexural strength) of the specimens was obtained.

Based on Table 2, it can be seen that the grout filling at the vertical interface between the corbel and the beam led to an increase of about 38% in the flexural strength between the LC and LS specimens and about 36% between PC and PS specimens. The main contribution attributed to this increase in strength was higher lever arm of internal tensile and compressive forces in negative bending section of the LC and PC specimens in relation to the LS and PS specimens.

Still based on Table 2, it can be noticed that the position of the continuity reinforcement (passing only in the slab or only in the

Table 2
Maximum applied loads and ultimate moment (flexural strength) of the connections

Specimen	F/2 (kN)	M _u (kN.m)
LC1	115.77	123.87
LC2	115.68	123.78
LS1	75.96	81.28
LS2	92.07	98.51
PC1	105.13	112.49
PC2	111.93	119.77
PS1	81.96	87.70
PS2	77.56	82.99

column) did not lead to relevant differences. The maximum bending moments achieved in LC specimens were about 6.6% higher than those achieved in PC specimens. Similarly, the LS specimens

achieved 5.3% higher ultimate moments than those achieved by the PS specimens.

3.3 Obtaining the moment-rotation curve

The bending moments at the connections were determined by Equation 1. The relative rotations were obtained by Equation 2 using the LVDTs readings shown in Figure 20.

$$M = \frac{F}{2} \times L \quad (1)$$

$$\theta = \frac{\text{mean}(2E/2D) + \text{mean}(4E/4D)}{390} \quad (2)$$

where

F is the load applied by the actuator;

L is the distance between the application point of the load and the column face (1.07 m);

M is the bending moment at the connection;

θ is the relative rotation between beam and column;

Table 3
Experimental determination of the flexural secant stiffness of the beam-column connections

Specimen	M _y (kN.m)	θ _y (rad)	Secant stiffness (kN.m/rad)	Mean secant stiffness (kN.m/rad)
LC1	106.65	0.0042969	24820	25525
LC2	106.62	0.0040647	26231	
LS1	55.517	0.017937	3095	3956
LS2	73.102	0.015178	4816	
PC1	105.51	0.0032868	32101	32256
PC2	110.99	0.0034244	32412	
PS1	72.957	0.013449	5425	6823
PS2	74.269	0.0090347	8220	

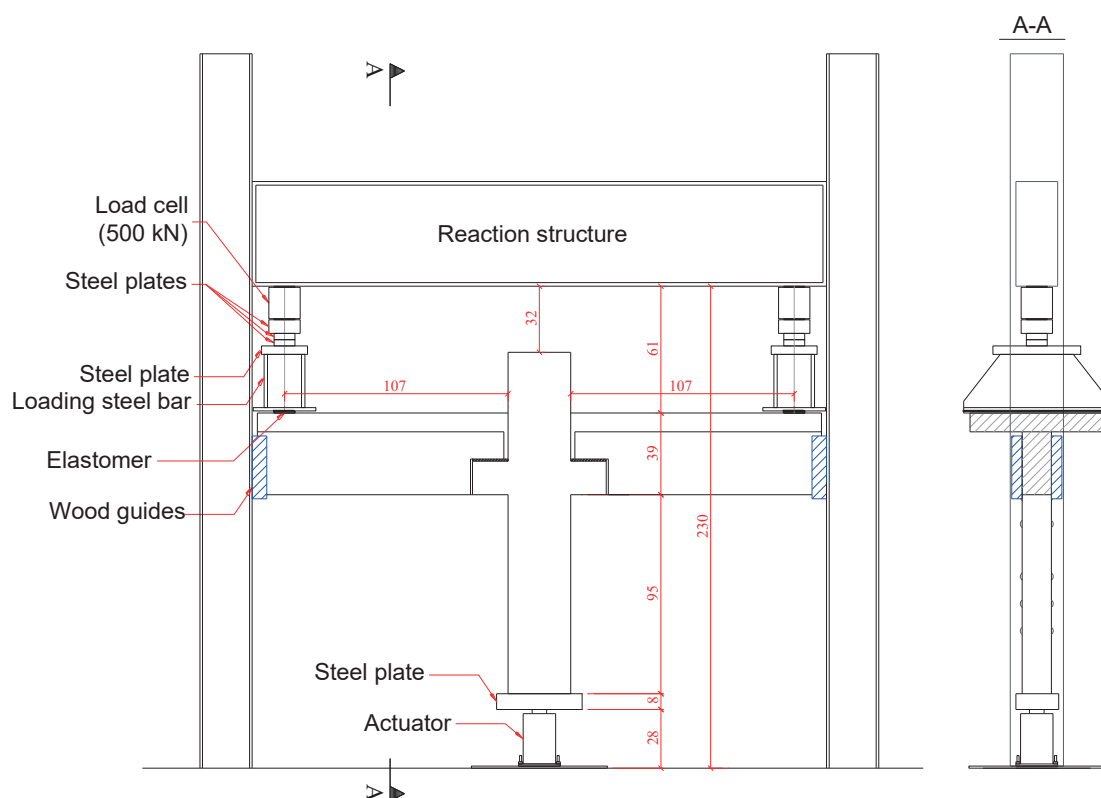


Figure 15
Test setup for the specimens and reaction structure (dimensions in cm)

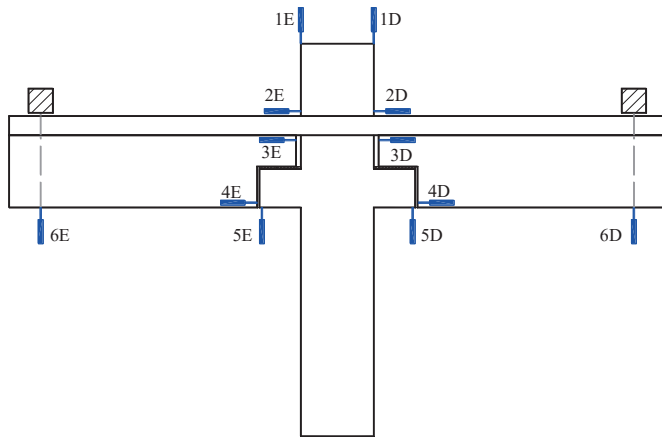


Figure 16
Position of the displacement transducers for all specimens



Figure 17
General view of the equipment used in the tests for measuring strains, displacements and loads



(a) Lc1 – front/left



(b) LC1 – front/right



(c) LS2 – front/left



(d) LS2 – front/right

Figure 18
Cracking pattern of the specimens LC and LS

2E, 2D, 4E and 4D are readings from the LVDTs 2E, 2D, 4E and 4D, respectively (in mm).

Figures 21 to 24 contain the experimental moment-rotation curves obtained with Equations 1 and 2. From these curves the parameters necessary to calculate the flexural secant stiffness (R_{sec}) were extracted, whose values are presented in Table 3.

In Table 3:

M_y is the bending moment corresponding to the beginning of yielding of the continuity reinforcement;

θ_y is the relative rotation corresponding to the beginning of yielding of the continuity reinforcement.

The results of Table 3 indicate that the grout filling at the vertical interface between the corbel and the beam contributed to the flexural stiffness increase of the connections. The average secant stiffness of LC specimens was about 6.5 times higher than the average secant stiffness of LS specimens. In turn, the average secant stiffness of PC specimens was about 4.7 times higher than the average secant stiffness of PS specimens.

Regarding the position of the continuity reinforcement, the specimens in which this reinforcement was crossing only in the column

presented higher flexural stiffness when compared to the specimens where the continuity reinforcement was crossing only in the slabs. The average secant stiffness of PC specimens was about 26.3% higher than the average secant stiffness of LC specimens. In turn, the average secant stiffness of PS specimens was about 72.5% higher than the average secant stiffness of LS specimens.

3.4 Experimental secant stiffness compared with simplified equation presented in Brazilian code NBR 9062 [27]

The updated Brazilian code for design of precast concrete structures - NBR 9062 [27] – provides a simplified equation for predicting the flexural secant stiffness of beam-column connections with continuity reinforcement in the negative bending moment region, according to Equation 3:

$$R_{sec} = k \frac{A_s E_s d^2}{L_{ed}} = k \frac{A_s E_s d^2}{\beta \phi + L_a} \quad (3)$$

where

A_s is the area of continuity reinforcement;

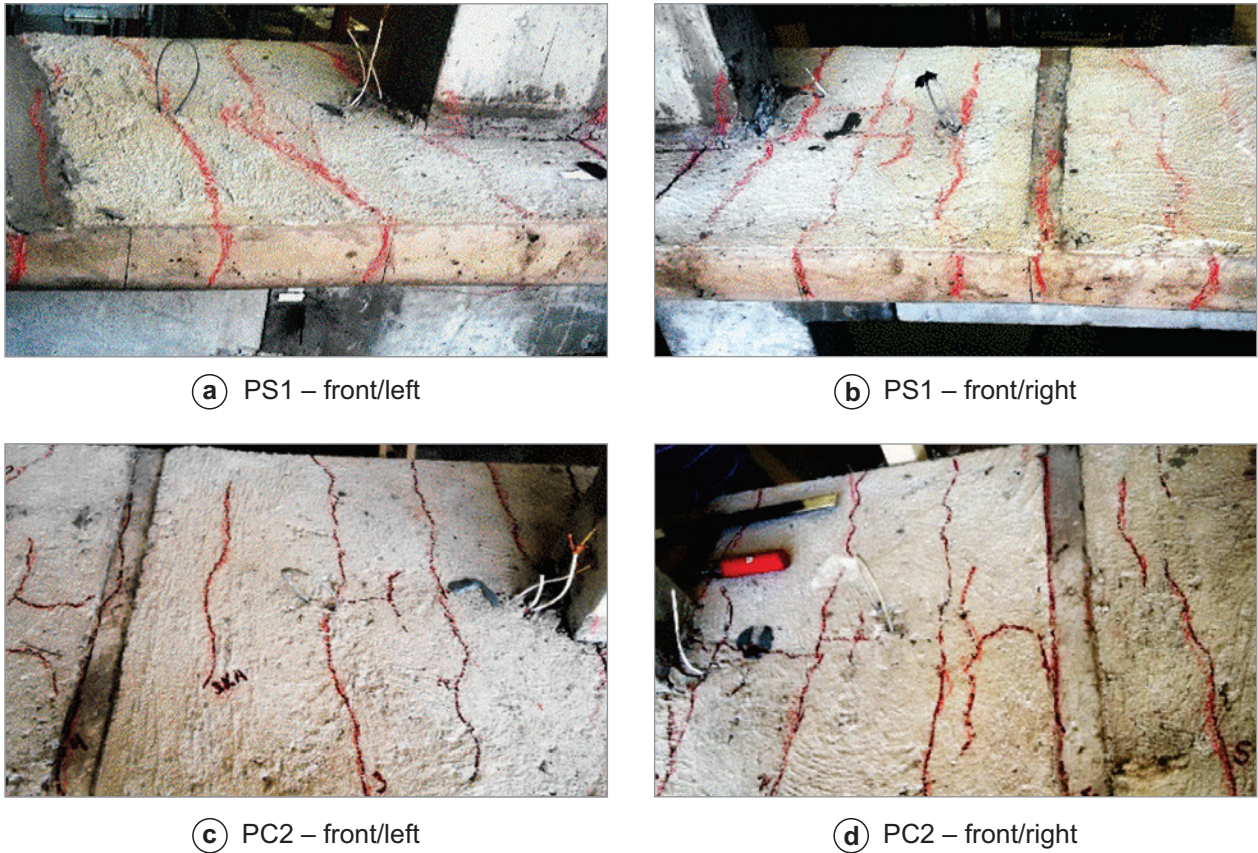


Figure 19
Cracking pattern of the specimens PS and PC

E_s is the modulus of elasticity of steel;
 d is the effective depth of the beam;
 L_{ed} is the effective deformation length related to elongation of the continuity reinforcement;
 ϕ is the diameter of the continuity reinforcement bars;
 L_a is the distance from the column face to the center of rotation (concrete corbel);

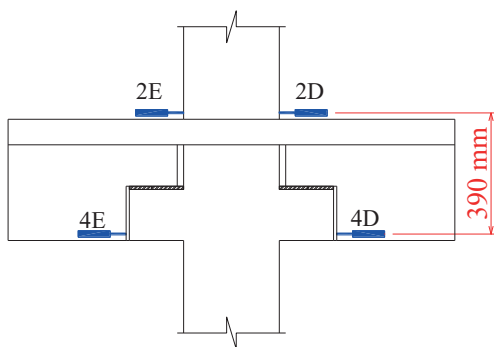


Figure 20
LVDTs used to determine relative rotations for all specimens

k is an adjustment coefficient for secant stiffness and β is a non-dimensional coefficient. Both coefficients depend on the type of connection.

NBR 9062 [27] presents the values k and β for two types of interior beam-column connections ($k=0.75$ and $k=1.0$; $\beta=25$ and $\beta=20$). However, the typologies investigated in this paper are not considered by the referred code. Thus, the secant stiffness and the coefficients k and β should be evaluated experimentally.

A procedure to evaluate the values of k and β is presented as follows, using the experimental results obtained for the PC and PS specimens. According to Ferreira *et al.* [28] and Ferreira [29], the relative rotation between beam and column is due to two deformation mechanisms. The first is related to the slippage of the continuity reinforcement inside the column (Mechanism A). The second mechanism is a consequence of the sum of the continuity reinforcement slips caused by cracks opening in the beam next to the column (Mechanism B). According to the FIB Guide [30], the slip of the continuity reinforcement inside the column (s_A) along the transmission length (l_t) in the elastic range can be calculated by:

$$s_A = \epsilon_s \left(\frac{\sigma_s}{\tau_b} \times \frac{\phi}{8} + 2\phi \right) \tag{4}$$

$$l_t = \frac{\sigma_s}{\tau_b} \times \frac{\phi}{4} + 2\phi \tag{5}$$

where

- ϵ_s is the strain of the reinforcement bar;
- σ_s is the stress of the reinforcement bar;
- τ_b is the average bond stress along the transmission length;
- ϕ is the steel bar diameter.

The average bond stress can be estimated by:

$$\tau_b = \sqrt{f_c} \quad (6)$$

where f_c is the concrete compressive strength of column (in MPa).

For all specimens investigated in this paper:

$$\sigma_s = f_y = 600\text{MPa} \quad f_c = 48\text{MPa} \quad \phi = 16\text{mm}$$

Thus, Equation 5 gives the following result for the transmission length at beginning of the yielding of the continuity reinforcement:

$$l_t = \frac{600}{\sqrt{48}} \times \frac{16}{4} + 2 \times 16 = 378\text{mm}$$

Since the maximum possible value for the transmission length is half the column depth ($0.5h_p = 0.5 \times 300 = 150\text{mm}$), the slip of continuity reinforcement bars cannot be calculated by Equation 4. How-

ever, assuming that the the steel stress and steel stain vary linearly along the transmission length $l_t = 0.5h_p$, it can be deduced the expression for the calculation of the slip by integrating the strain of steel bar:

$$s_A = \epsilon_s \left[0.5h_p - 2 \frac{\tau_b}{\sigma_s} \times \frac{(0.5h_p - 2\phi)^2}{\phi} \right] \quad (7)$$

Considering $E_s = 210\text{GPa}$ for the modulus of elasticity of steel, the slip associated with the first deformation mechanism (Mechanism A) corresponding to the beginning of the yielding of the continuity reinforcement is calculated by:

$$s_{y,A} = \frac{600}{210000} \left[0.5 \times 300 - 2 \frac{\sqrt{48}}{600} \times \frac{(0.5 \times 300 - 2 \times 16)^2}{16} \right] = 0.3711\text{mm}$$

The slip (s_B) related to the formation of flexural cracks at the beam end next to the joint region (Mechanism B) can be evaluated by Alva and El Debs [31]:

$$s_B = \epsilon_s \frac{(L_p + s_R)}{2} \quad (8)$$

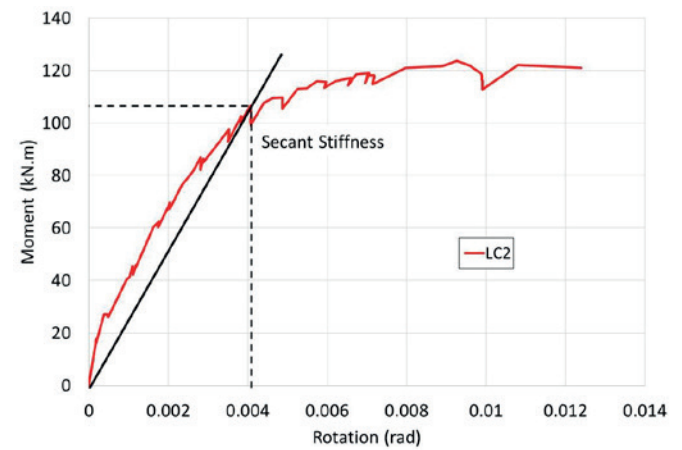
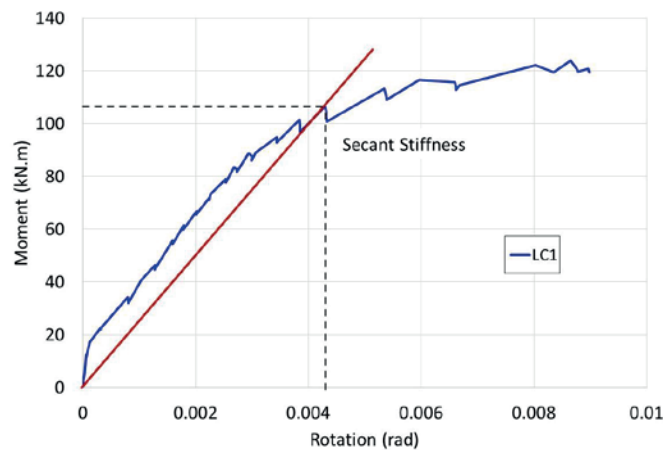


Figure 21
Moment-rotation curve: specimens LC1 and LC2

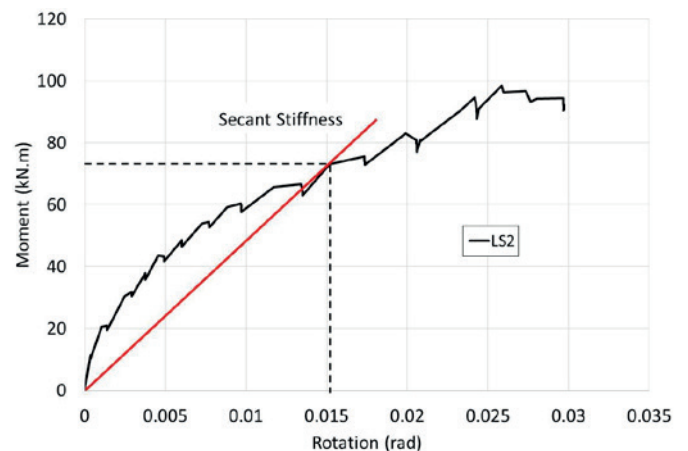
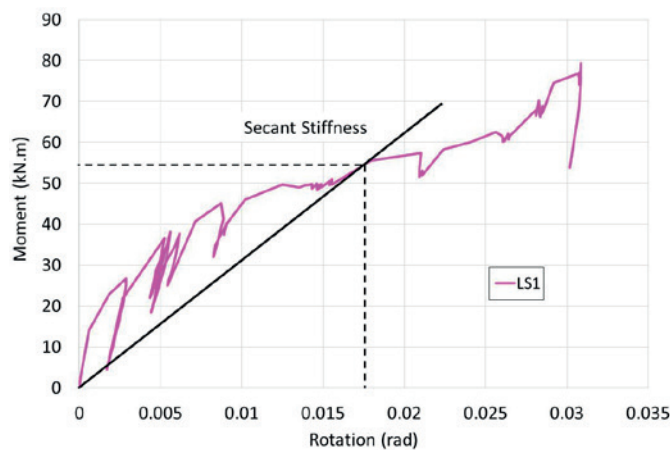


Figure 22
Moment-rotation curve: specimens LS1 and LS2

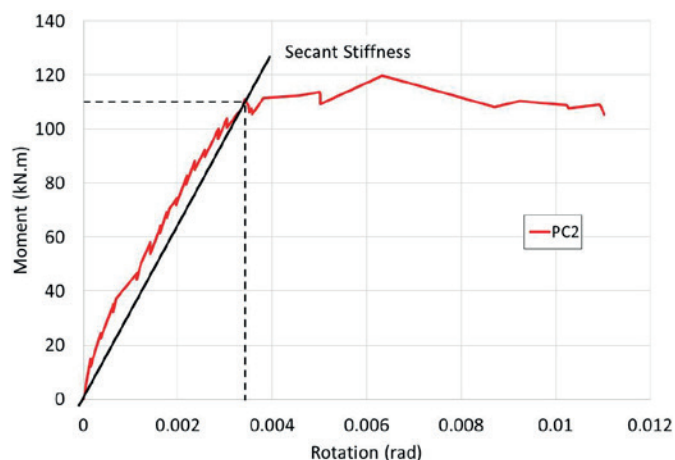
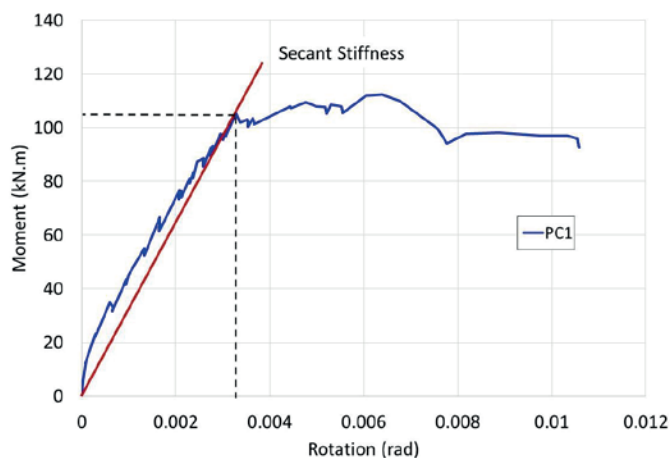


Figure 23
Moment-rotation curve: specimens PC1 and PC2

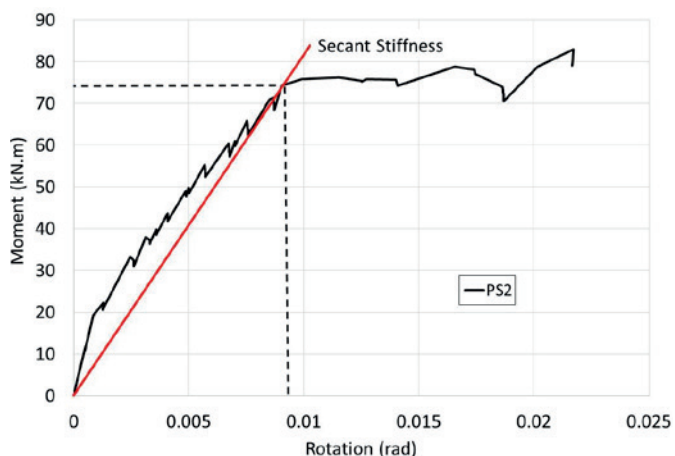
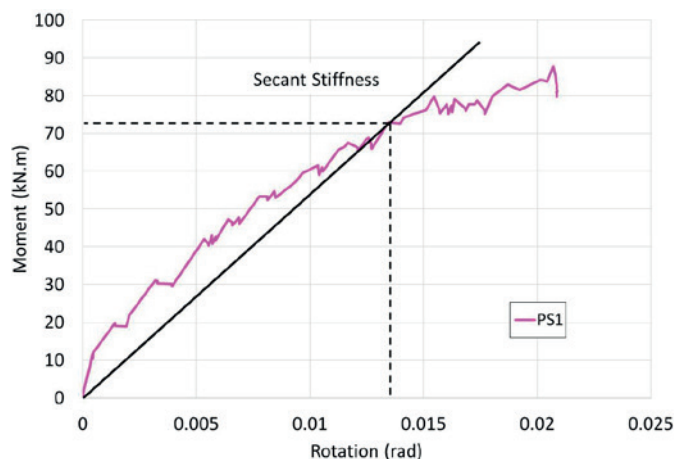


Figure 24
Moment-rotation curve: specimens PS1 and PS2

where

L_p is the plastic hinge length (where is higher concentration of cracks in the connection region);

s_R is the crack spacing.

According to Paulay and Priestley [32], a good estimate of the plastic hinge length for a cantilever beam may be obtained by:

$$L_p = 0.08L + 0.022 \times \phi \times f_y \tag{9}$$

where

L is the span of the beam (in meters). For the specimens investigated: $L = 1.07\text{m}$;

ϕ is the steel bar diameter (in meters). For the specimens investigated: $\phi = 0.016\text{m}$;

f_y is the yield stress of reinforcement steel (in MPa). For the specimens investigated: $f_y = 600\text{MPa}$.

Substituting values in Equation 9:

$L_p = 296.80\text{mm}$ (for all specimens)

The crack spacing (s_R) may be evaluated from code expressions,

such as Equation 10 presented in Eurocode 2 [33]:

$$s_R = k_3 c + k_1 k_2 k_4 \frac{\phi}{\rho_{s,\text{eff}}} \tag{10}$$

where

c is the concrete cover;

$$\rho_{s,\text{eff}} = \frac{A_s}{A_{c,\text{eff}}}$$

A_s is the area of reinforcing steel in the tensile zone;

$A_{c,\text{eff}}$ is the effective area of concrete in tension surrounding the reinforcement;

$k_1=0.8$ $k_2=0.5$ $k_3=3.4$ $k_4=0.425$.

For all specimens: $c = 22\text{mm}$ and $A_s = 4.02\text{cm}^2$.

For specimens PC: $A_{c,\text{eff}} = 105.00\text{cm}^2$, $\rho_{s,\text{eff}} = 0.0383$ and $s_R = 145.85\text{mm}$

For specimens PS: $A_{c,\text{eff}} = 72.44\text{cm}^2$, $\rho_{s,\text{eff}} = 0.0555$ and $s_R = 123.81\text{mm}$

Thus, at the beginning of yielding of the continuity reinforcement,

Equation 8 gives:

Specimens PC:

$$s_{y,B} = \frac{600}{210000} \left(\frac{296.80 + 145.85}{2} \right) = 0.6324 \text{mm}$$

Specimens PS:

$$s_{y,B} = \frac{600}{210000} \left(\frac{296.80 + 123.81}{2} \right) = 0.6009 \text{mm}$$

Therefore, the total slip induced by the two mentioned deformation mechanisms is:

Specimens PC:

$$s_y = s_{y,A} + s_{y,B} = 0.3711 + 0.6324 = 1,0035 \text{mm}$$

Specimens PS:

$$s_y = s_{y,A} + s_{y,B} = 0.3711 + 0.6009 = 0.9720 \text{mm}$$

Since the effective deformation length L_{ed} is related to elongation of the continuity reinforcement, the following relationship at the beginning of yielding of the continuity reinforcement can be established:

$$\epsilon_y = \frac{s_y}{L_{ed}} \quad (11)$$

$$L_{ed} = \frac{s_y}{\frac{f_y}{E_s}}$$

For specimens PC:

$$L_{ed} = \frac{1,0035}{\frac{600}{210000}} = 351.23 \text{mm} = 35.123 \text{cm}$$

For specimens PS:

$$L_{ed} = \frac{0,9720}{\frac{600}{210000}} = 340.20 \text{mm} = 34.020 \text{cm}$$

The experimental values k and β in Equation 3 are obtained from experimental values of flexural stiffness (see Table 3).

For specimens PC:

$$32256 \times 10^2 = \frac{k \times 4.02 \times 21000 \times 36^2}{35.123} \rightarrow k = 1.036$$

$$35.123 = \beta \times 1,6 + \frac{17}{2} \rightarrow \beta = 16.64$$

Likewise, the experimental values of the coefficients k and β are evaluated for specimens PS:

$$6823 \times 10^2 = \frac{k \times 4.02 \times 21000 \times 19^2}{34.020} \rightarrow k = 0.762$$

$$34.020 = \beta \times 1,6 + \frac{17}{2} \rightarrow \beta = 15.95$$

4. Conclusions

Based on the experimental results presented in this paper, the following conclusions can be highlighted:

- For both the specimens in which the entire continuity reinforcement has crossed the column and also for the specimens where this continuity reinforcement has been distributed only to the slab, the grout filling at the vertical interface between the corbel and beam contributed to increase the flexural strength of the connection in values slightly above 30% in relation to the prototypes without filling. This is due to the increase of the lever arm of internal tensile and compressive forces in beam cross section at the connection region;

- Grout filling at the vertical interface between the corbel and beam contributed significantly to increase the bending stiffness of the connections. In specimens where the whole continuity reinforcement crossed the column, the secant flexural stiffness was about 5 times higher than the prototype stiffness without filling. In specimens that the entire continuity reinforcement was distributed only on the slab, the secant flexural stiffness was about 6.5 times higher than the prototype stiffness without filling. This is because the existing free space between the corbel and beam in specimens PS and LS allows greater rotational freedom in these connections;
- In terms of flexural strength, the results indicated that the connections with the continuity reinforcement crossing only the slab and crossing only the column are similar, that is, no significant differences were found between the strength of the connections due to the positioning of the reinforcement continuity. This finding refers to both specimens with vertical grout filling and specimens without such grout;
- For the same amount of continuity reinforcement, the specimens in which this reinforcement only crossed the columns showed higher flexural stiffness than the specimens in which this reinforcement only passed in the slabs: PC about 26% higher than the LC and PS about 72% higher compared to LS;
- The benefit/cost ratio resulting from the increased difficulty to perform vertical grout filling in the analyzed typologies is high, considering the gains obtained in terms of flexural strength and flexural stiffness of the connections;
- The non-dimension coefficients k and β used to calculate the flexural secant stiffness of the connection in the expression proposed by NBR 9062 (2017) were evaluated from the experimental results for the two connection types investigated (PS and PC), which are not yet covered by that code. In turn, the values obtained for these coefficients in this study can be useful as indicative and guiding values for structural designers or useful for future research on the subject.

5. Acknowledgments

To CAPES for financial support to the second author and to Legran Engenharia for supplying the precast beams and columns used in the tests.

To CNPq for financial support to the first autor (Process: 308720/2018-0).

6. References

- [1] DOLAN, C. W.; STANTON, J. F.; ANDERSON, R. G. Moment resistant connections and simple connections. *PCI Journal*, v.32, n.2, p.62-74, 1987.
- [2] SECKIN, M.; FU, H. C. Beam-column connections in precast reinforced concrete construction. *ACI Structural Journal*, v.87, n.3, p. 252-261, 1990.
- [3] GORGUN, H. Semi-rigid behaviour of connections in precast concrete structures. Thesis (Department of Civil Engineering)-University of Nottingham, United Kingdom, 1997.
- [4] ALCOCER, S.M; CARRANZA, R.; PEREZ-NAVARRETE, D.; MARTINEZ, R. Seismic tests of beam-to-column con-

- nections in a precast concrete frame. *PCI Journal*, v.47, n.3, p.70-89, 2002.
- [5] KHALOO, A.R.; PARASTESH, H. Cyclic loading response of simple-moment resistant precast concrete beam-column connection. *ACI Structural Journal*, v.100, n.4, p. 440-445, 2003.
- [6] KHALOO, A.R.; PARASTESH, H. Cyclic loading response of precast concrete beam-column connection. *ACI Structural Journal*, v.100, n.3, p. 291-296, 2003.
- [7] ERTAS, O.; OZDEN, S.; OZTURAN, T. Ductile connections in precast concrete moment resisting frames. *PCI Journal*, v.51, n.3, p.66-76, 2006.
- [8] HASAN, S.A. Behaviour of discontinuous precast concrete beam-column connections. Thesis (Department of Civil Engineering)-University of Nottingham, United Kingdom, 2011.
- [9] CHOI, H.-K; CHOI, Y.-C; CHOI, S.-C. Development and testing of precast concrete beam-to-column connections. *Engineering Structures*, 2013, 56:1820-1835.
- [10] IM, H.-J.; PARK, H.-G; EOM, T.-S. Cyclic loading test for reinforced-concrete-emulated-beam-column connection of precast concrete moment frame. *ACI Structural Journal*, v.110, n.1, p. 115-125, 2013.
- [11] PARASTESH, H.; HAJIRASOULIHA, I.; RAMEZANI, R. A new ductile moment-resisting connection for precast concrete frames in seismic regions: An experimental investigation. *Engineering Structures*, 2014, 70:144-157.
- [12] YUKSEL, E.; KARADOGAN, H.F.; BAL, I.E.; ILKI, A.; BAL, A.; INCI, P. Seismic behavior of two exterior beam-column connections made of normal-strength concrete developed for precast construction. *Engineering Structures*, 2015, 99:157-172.
- [13] GUAN, D.; GUO, Z.; XIAO, Q.; ZHENG, Y. Experimental study of a new beam-to column connection for precast concrete frames under reversal cyclic loading. *Advances in Structural Engineering*, 2016, v.19, n.3, p.529-545.
- [14] BAHRAMI, S.; MADHKHAN, M.; SHIRMOHAMMADI, F.; NAZEMI, N. Behavior of two new moment resisting precast beam to column connections subjected to lateral loading. *Engineering Structures*, 2017, 132:808-821.
- [15] SOARES, A.M.M. Análise estrutural de pórticos planos de elementos pré-fabricados de concreto considerando a deformabilidade das ligações. 181 p. Dissertação (Mestrado) – Departamento de Engenharia de Estruturas, Escola de Engenharia de São Carlos, Universidade de São Paulo, 1998.
- [16] FERREIRA, M. A. Deformabilidade de ligações viga-pilar de concreto pré-moldado. 232 p. Tese (Doutorado) – Departamento de Engenharia de Estruturas, Escola de Engenharia de São Carlos, Universidade de São Paulo, 1998.
- [17] MIOTTO, A.M. Ligações viga-pilar de estruturas de concreto pré-moldado: análise com ênfase na deformabilidade ao momento fletor. 234 p. Tese (Doutorado) – Departamento de Engenharia de Estruturas, Escola de Engenharia de São Carlos, Universidade de São Paulo, 2002.
- [18] SOUZA, A.S. Comportamento de elementos pré-moldados de concreto com ligações semi-rígidas. 99 p. Dissertação (Mestrado) – Universidade Federal de São Carlos, São Carlos, 2006.
- [19] BALDISSERA, A. Estudo experimental de uma ligação viga-pilar de concreto pré-moldado parcialmente resistente a momento fletor. 149 p. Dissertação (Mestrado) – Departamento de Engenharia de Estruturas, Escola de Engenharia de São Carlos, Universidade de São Paulo, 2006.
- [20] KATAOKA, M.N. Estrudo da continuidade em ligações laje-viga-pilar em estruturas pré-moldadas de concreto. 113 p. Dissertação (Mestrado) – Universidade Federal de São Carlos, São Carlos, 2007.
- [21] MOTA, J.E. Contribuição ao projeto de estruturas multipiso reticuladas em concreto pré-moldado. 246 p. Tese (Doutorado) – Departamento de Engenharia de Estruturas, Escola de Engenharia de São Carlos, Universidade de São Paulo, 2009.
- [22] SAWASAKI, F.Y. Estudo teórico-experimental de ligação viga-pilar com alfomada de argamassa e chumbador para estruturas de concreto pré-moldado. 188 p. Dissertação (Mestrado) – Departamento de Engenharia de Estruturas, Escola de Engenharia de São Carlos, Universidade de São Paulo, 2010.
- [23] TROTTA, A.M. Estudo experimental de uma ligação viga-pilar em concreto pré-moldado utilizando perfis metálicos e solda. 101 p. Dissertação (Mestrado) – Departamento de Engenharia de Estruturas, Escola de Engenharia de São Carlos, Universidade de São Paulo, 2012.
- [24] BACHEGA, L.A. Estudo teórico-experimental de ligação viga-pilar com consolo metálico embutido em estruturas pré-moldadas de concreto. 146 p. Dissertação (Mestrado) – Universidade Federal de São Carlos, São Carlos, 2013.
- [25] HADADE, M.A.S. Comportamento de ligações viga-pilar típicas com continuidade de armadura negativa em estruturas pré-fabricadas. 243 p. Tese (Doutorado) – Universidade Federal de São Carlos, São Carlos, 2016.
- [26] LACERDA, M. M. S. Análise da influência do grauteamento e da posição das armaduras na ligação viga-pilar em estruturas de concreto pré-moldado. 171 p. Dissertação (Mestrado) - Faculdade de Engenharia Civil, Universidade Federal de Uberlândia, 2016.
- [27] ASSOCIAÇÃO BRASILEIRA DE NORMAS TÉCNICAS. NBR 9062: Projeto e execução de estruturas de concreto pré-moldado. Rio de Janeiro: ABNT, 2017.
- [28] FERREIRA, M.A; ELLIOTT, K.S.; HASAN, S.A. Precast Concrete Framed Structures with Semi-Rigid Connections. State of Art Research Report. School of Civil Engineering, University of Nottingham, 2010.
- [29] FERREIRA, M.A. Analytical Design Procedure for Semi-Rigid Connections in Precast Concrete Structures. Research Report, School of Civil Engineering, University of Nottingham 2001.
- [30] FÉDERATION INTERNATIONALE DU BÉTON. FIB - Bulletin 43: Structural connections for precast concrete buildings. Guide to good practice, 2008.
- [31] ALVA, G.M.S; EL DEBS, A.L.H.C. Moment-rotation relationship of RC beam-column connections: experimental

tests and analytical model. *Engineering Structures*, 2013, 56:1427-1438.

- [32] PAULAY, T.; PRIESTLEY, M.J.N. *Seismic Design of Reinforced Concrete and Masonry Buildings*. New York: John Wiley & Sons, 1992.
- [33] EUROPEAN COMMITTEE FOR STANDARDIZATION. *Eurocode 2: Design of Concrete Structures – Part 1: General Rules and Rules for Building*. Brussels, 2004.